A new methodology to analyse and optimize territorial compensations of solar radiation intermittency: A case study in Corsica Island (France)

Pierrick Haurant, M. Muselli, L. Gaillard, P. Oberti

A new methodology to analyse and optimize territorial compensations of solar radiation intermittency: a case study in Corsica Island (France)

Haurant P.[a,1,*], Muselli M.[b], Gaillard L.[c], Oberti P.[d]

[a] *IMT Atlantique, GEPEA, UMR CNRS 6144, F-44307 Nantes, France*
[b] *Université de Corse Pasquale Paoli, Avenue du 9 septembre, BP 52, 20250 Corte, France*
[c] *Heliocity SAS, 31 rue Gustave Eiffel, 38000 Grenoble, France*
[d] *Université de Corse Pasquale Paoli, UMR CNRS 6240 LISA, Av. Jean Nicoli, 20250 Corte, France*

Abstract

Territorial compensations of variability are a lever for smoothing the global photovoltaic production. They may allow a higher penetration rate of photovoltaic production in an energy mix, especially for non-interconnected islands. The aim of this paper is to analyse and optimise the smoothing effects of solar resource on a territory. In that view a novel typological classification-based methodology is proposed: intervals from highly intermittent episodes to ones with few fluctuations are discriminated. Then, the potential for compensation is demonstrated through the transformation from classes of high to low variability when summing solar radiation over several sites instead of one alone. The methodology is applied to Corsica. Solar radiation measured at 1 Hz on 8 sites which criss-crosses the island, when summed, demonstrates a reduction in the set of most intense variations compared to individual basis: they represent 5.5 % to 15.5 % of the studied period for the sites taken individually against only 1.7 % for the cumulated radiation. Optimisation of the territorial compensation strategy leads to a near-disappearance of intense variations, with this class representing only 0.13 % of the period. Finally, the optimized dispersion map of solar capacities results from this optimisation.

Keywords: Solar radiation, Classification, Variability, Territorial compensations, Smoothing effect, Optimization

*Corresponding author

Nomenclature

$_{inter}$	Inter-interval	$\mathbb{I}$	Interval
$_{intra}$	Intra-interval	b	Classification thresholds [s]
$_{S_i}$	Refers to site S_i	C	Class
$_{t_{tot}}$	Refers to t_{tot}, the studied period	d	Distances between sites [km]
$_{t_{var}}$	Refers to t_{var}	F	Objective function [s]
$_{tot}$	Refers to total (or cumulated)	G	Global horizontal radiation [$\mathrm{W\,m^{-2}}$]
$_{var}$	Variable	k_b	Direct fraction
β	Weight coefficient	k_t	Clarity index
λ	Longitude [°]	k_{cls}	Clear sky index
φ	Latitude [°]	N	Number (sites, instants)
δG	Relative variation of radiation [s]	P_N	Relative total number of intervalles [%]
δt	Variation scale [s]	P_t	Relative cumulated interval duration [%]
		r	Pearson correlation coefficients [-]
		S	Site
		t	Time [s]

1. Introduction

Multicriteria selection of potential photovoltaic (PV) plants in Corsica revealed the challenges associated to the territorial concentration of grid-connected plants [1, 2]. Of primary concern is the abrupt loss in energy generation arising from localized heavy cloud cover. The issue is part of the broader challenge of resource intermittency, which has been extensively studied for the electricity infrastructures with a high penetration of photovoltaic technology [3, 4, 5, 6]. The risk of grid instability has resulting in a limit being set on the amount of installed capacity that can be based on intermittent renewable sources. This limit can be highly constraining particuliarly for small grids such as non-interconnected islands. For instance, for the islands of La réunion and Corsica (France), this limit was set to 35 % of total electrical power by decrees [7, 8].

Today this regulatory constraint is a significant limiting factor for the transition to renewable energy technologies such as photovoltaic facilities, which may only progress if the technical feasibility of safely exceeding the limit can be proven. Small grids in non-interconnected zones such as on islands are especially impacted by this limit. In this context, the intermittence of the solar resource, its territorial variations and its predictability stand as major issues for the energy utility operator. A good knowledge of the solar resource variation over a territory would enable territorial compensation strategies to smooth photovoltaic generation as suggested by [9] and thereby allow the limit on renewable integration to be increased.

The spatial variability of solar radiation is typically shown through the analysis of inter-sites Pearson correlation coefficients r presented as a function of the distances between the studied sites [10, 11, 12, 13, 14]. A more advanced treatment was introduced by [15] and [16] who defined the discorrelation distance as the distance for which r drops below 0.5. Other authors have proposed statistical indices with which to compare fluctuations of solar radiation at various sites. For instance, [12] studied the standard deviation of hourly clearsky k_{cls} between 2 sites, obtained with satellite data. [10] discussed the solar radiation

difference between two sites by comparing the difference to the mean daily value of solar radiation. [17] compared solar radiation power spectra of several sites, and focused particuliarly on the linear best fit line for time scales less than 1 h.

The spatial variability of solar radiation demonstrated though the discorrelation between sites induces shifts in temporal fluctuations from a site to other. Thus for a given period, statistical compensations of variations can be expected on a territory. These spatial compensations are exposed and analysed in various studies. [17] examined the average smoothing effect of solar radiation received by 4 sites separated by several tens of kilometres (20 km to 180 km), at different time scales. The ramp rate analysis of the average revealed a significant decrease in their mean and maximum magnitude, standard deviation, and kurtosis compared to each site individually. Also, probability distribution functions and cumulative distribution functions of ramp rates indicated that the average of all four sites is less likely to have large fluctuations than each of the other sites individually. Similiarly, [15] compared boxplots of 1 Hz measurements at 7 isolated sites on the island of La Réunion to their aggregated radiation. The averaged radiation variability showed narrower distributions than individual stations, with less hour-to-hour variability. The spatial smoothing of the solar potential was shown to exist for a small geographic site in Japan by [18]. In that work, the mean value of a network of 9 pyranometers covering a 4 km by 4 km area was found to fluctuate to a significantly lesser degree than the individual readings of each sensor.

Spatial compensations on solar radiation smooth the PV generation that allows a better integration in the energy mix. At PV plants scale first, [19] analysed the PV output of 6 plants of different sizes, from 0.2 ha to 52 ha, scattered over a 1000 km^2 area in the south of Navarra (Spain). Smoothing of power fluctuations has demonstrated for large PV plants, and this effect is particularly noticeable for small time steps. At larger scale, [20] performed a multi-objective optimization, maximizing energy and minimizing variability, to allocate 2 MW PV among four sites, with differing amounts at each site, on the island of Lanai, Hawaii. For the optimal allotment, the variability in

the form of ramp rates, were reduced by 50 %, whereas energy was reduced by only 3 % over the maximum production case. [21] have shown that the dispersal of PV installations over a wide territory can enable a higher degree of penetration of PV systems without jeopardizing grid stability, from 1.3 % for a fully centralized facility to 37 % for a distributed system covering 1000 km^2. Also, [22] studied how geographic dispersion of PV installations may minimize electricity supply uncertainty in Virginia (USA). They showed the probabilities of generation shortfalls was lowered for decentralized configurations, since the variability of the production are less variable.

Thus, the smoothing effects on solar radiation over a territory, when it is demonstrated, is a lever to limit the intermittence of the global photovoltaic production. Consequently, the territorial compensations of solar radiation offer a mean to increase the deployment of renewable energy technologies. These compensations are already analysed with statistical tools at different scales and territories in the literature. However no method has been proposed neither to quantified the smoothing effect of the solar radiation, nor to build a roadmap for an optimal dispersion of PV installation over a wide territory.

This paper addresses these two issues through a novel methodology for the analysis and optimization of the territorial compensations of radiation variability. The methodology is based on the classification of solar radiation variability and the quantification of durations of intermittent classes. The optimization consists then in finding the dispersion of PV capacity that minimizes the duration of the most intermittent class. To treat these issues, the main novelties of the paper are the following :

- A new typological classification methodology of solar radiation variations
- The use of a typological classification for studying the temporal variability of solar resource over measurement sites
- The application of the typological classification for analysing and quantifying the smoothing effects on solar radiation over a territory

- The optimization of the smoothing effect for minimizing the intermittence of PV production

The paper is structured with four sections: the overall methodology, based on typological classification and optimisation of territorial compensations of variation, is introduced in section 2. A case study comprising several different sites is described in section 3. Finally, results of the metholodogy applied to the case study are presented in section 4. Solar ressource variations of individual sites, as well as considering them altogether are qualified and classified. Finally, the presence of territorial compensations is demonstrated and then these are optimised for the dataset.

2. Methodology

2.1. Classification methodology

If source intermittency is well understood, periods of deficient solar energy can be mitigated by managing the various energy generation plants at the disposal of the utility operator. As a first step towards developing effective strategies to overcome intermittency, it is important to develop a means to characterise the feature in a rigorous manner using data with a sampling time short enough to capture rapid fluctuations in radiation intensity.

Temporal fluctuation of solar resource is usually characterized by the analysis of statistics on timeseries of solar radiation or photovoltaic generation data. [12] calculated standard deviation of PV production measured at various times steps. [15] used boxplots of k_{cls} to describe distributions of this index via their median, 1^{st} and 3^{rd} quartiles. [13] applied autocorrelation coefficients presented as a function of different temporal lags. Moreover, ramp rates are also analysed through their probability densities, cumulative probabilities functions [17], power spectral analysis [23, 17] and counting of ramp rates occurrences over a given threshold [19].

Irradiance measurements for multiple sites spanning a sufficient period with a high sampling frequency leads to a significant volume of data to analyse. Rather

than conventional statistical tools, typological classifications can prove advantageous. Within this framework, a classification methodology was developed to identify and describe the nature of variations in solar radiation for individual sites in order to demonstrate the spatial compensations phenomenon.

The typological classification of solar radiation per day or instantaneously has been previously studied for satellite image processing [24, 25], the decomposition of total radiation into its direct and diffuse components [26] or the calculation of radiation incident on an inclined plane. Typically, within such studies, periods are classified into intervals of clear sky, partial cloud or overcast conditions, so that different models can be applied to each scenario. The segregation of a data into two or three intervals using instantaneous indicators of cloud cover or sky clarity provides a first means of classification. Thanks to its simplicity, this approach has been widely implemented in previous works [27, 28, 26, 24, 25]. However, since it evokes a static measure of daily cloudy conditions, the method is incapable of retaining dynamic information such as the degree of variability of cloud cover. Hence, a highly variable day can be attributed the same indicator of mean clarity as an overcast day.

Other typological methods allow the dynamics of passing clouds to be taken into account: the categorization by the mean clarity index k_t was complemented by mathematical quantities to quantify the roughness of the signal such as the fractal dimension [29, 30] or the Dirichlet coefficients [31] or wavelet decomposition coefficients [32].[33] classified the daily distribution of direct fraction k_b time series at reduced time-step. The methodology consists in combining three data mining methods: principal component analysis (PCA), K-means clustering methods and Ward hierarchical method to determine five typical days at La Réunion Island. [34] used a set of discrimination parameters derived from hourly clarity index k_t to define three types of day in Corsica, applying Ward hierarchical method. The dynamics of solar radiation were taken into account through an integral of the square of the second derivative of k_t. Similarly, [15] identified five different solar radiation regimes at La Réunion, using k-means clustering analysis. They considered the irradiance level with the daily clear

sky index and the variability through two parameters:

1. a Total Relative Change (TRC) of the clear sky index between 10 h and 16 h
2. a Random Absolute Relative Change (RARC) index that represents the sum of short-term variability, excluding the variability trend of the day.

These recent methods, less trivial and more satisfactory represent nevertheless the limitation of classifying days by averaging over instantaneous indicators, despite the fact that even within a single day it is possible to observe periods of different weather conditions. Once again, the characteristics of each weather phenomenon becomes smoothed and attenuated and, consequently distinctly different days may become embroiled together. Therefore, the categories represent a large number of different radiation profiles. An additional shortcoming is their limitation to the classification of complete days rather than short intervals. In this respect, these methods are inadequate for the electricity utility operator who must be able to forecast the intra-day conditions for energy generation. To break away from this limitation, days may instead be considered as successions of sunlight regimes to be identified by a suitable classification algorithm. The typological classification method of solar radiation variability by interval, mentioned in [35] is presented in a comprehensive manner in this paper.

2.1.1. Variation scale

Regimes in solar radiation distinguish themselves in particular by the form of the variations in irradiance that are observed, which can be characterized by two criteria: their duration and amplitude. The objective of this work is to develop a classification method of the regimes according to these properties.

The variation scale refers to the duration of time intervals for which the variation of solar radiation is evaluated. It is duration between two consecutive instants for which the relative variation δG is calculated, ignoring the variations present in the interval, following the relation:

$$\delta G(t) = \left| \frac{G(t) - G(t - \delta t)}{G(t - \delta t)} \right| \quad (1)$$

2.1.2. Categories of variations

Different solar radiation variation dynamics are discriminated by the variation scales. In effect, variations that are too slow to be perceived for a given δt can be revealed for larger time intervals (Fig. 1).

For a given day, if the data points with a variation greater than 10 % are selected, one observes that four discontinuous and relatively short groups are revealed for a variation scale of $\delta t = 1\,\mathrm{s}$, corresponding to times when the solar radiation fluctuates considerably. A large set of points is identified for a variation scale of $\delta t = 300\,\mathrm{s}$, and indeed it is observed that low frequency variations occurring between 3:00 pm – 5:00 pm are particularly considered. Finally, nearly all points in the interval 12:45 – 5:20 pm are recovered when $\delta t = 1200\,\mathrm{s}$. The scales of variation therefore render visible and quantifiable the intensity of the variability following the rule according to which, the smaller the δt beyond which the variations become visible, the stronger and tighter the variations.

It is therefore possible to construct a typology on the basis of scales of variations according to the following procedure: considering the scales retained, calculate and compare the variations for a threshold in variability. The variations superior to this threshold are associated to the equivalent class, which can be semantically defined as a class of "variations visible at such a scale". Two distinct scales δt_1 and δt_2 give rise to three classifications, including the class of negligible variations. It is useful to choose scales that are separated by several orders of magnitude, in order to categorize qualitatively different variation profiles.

2.1.3. Delimitation of intervals

For most cases, even within a highly active cloudy regime, variations of solar radiation are found to only occasionally exceed the fixed threshold. The

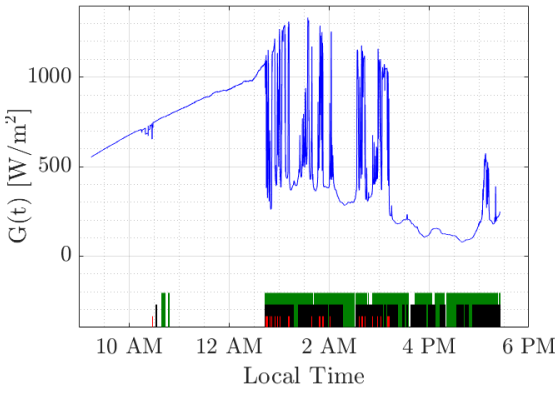

Figure 1: Variations revealed by different values of variations scales : $\delta t = 1\,\mathrm{s}$ in red, $\delta t = 300\,\mathrm{s}$ in black and $\delta t = 1200\,\mathrm{s}$ in green

categorization condition therefore generates a large number of instants of different classes that pass in rapid succession. On the other hand, an isolated and punctual variation, as may arise from a single passing cloud for example, may generated an isolated micro-interval. It seems therefore important to regroup these micro-intervals into large interval. The definition of criteria with which to regroup the data is therefore needed in order to limit the number of entities, whist respecting the similarity of variation profiles that have been regrouped.

The two filters have been introduced following this rational. The first threshold represented the maximum duration between two variations so that they are regrouped into the same interval. Labelled b_{intra}, it is the intra-interval threshold. The second threshold compares to a minimum duration of intervals: it is the inter-interval threshold b_{inter}. Using these two thresholds, the following four-steps sequential procedure (Fig.2)

1. Variable instants t_{var} are identified as instants for which the variations of solar radiation exceed the threshold of variability b_{var} (Step 0 & 1):

$$t_{var} = \{t \text{ s.t. } \delta G(t) \geq b_{var}\} \tag{2}$$

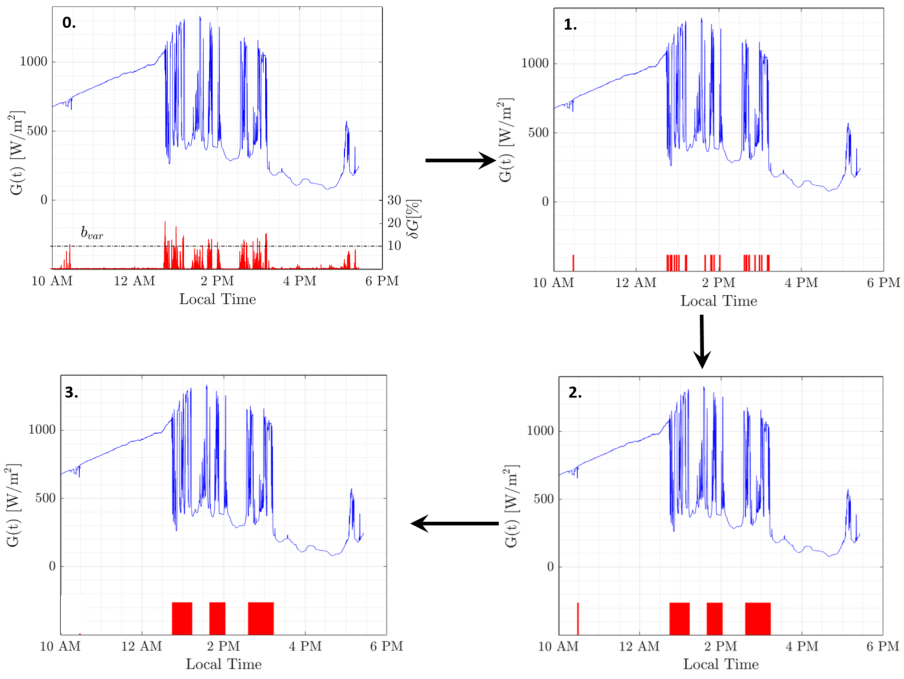

Figure 2: Diagram of the method : 0.&1. Identification of variations ($b_{var} = 0.1$) ; 2. Intra-interval grouping step ($b_{intra} = 900\,\mathrm{s}$) and 3. inter-interval grouping step ($b_{intra} = 900\,\mathrm{s}$) (measured irradiance at Corte, 24$^{\mathrm{th}}$ May 2010)

2. Times between two distinct variations separated by an interval which duration do not exceed the threshold b_{intra} are in turn considered : this step comprises the inter-interval regrouping, or the homogenisation during which the set of fluctuating irradiance intervals $\mathbb{I}_{var}$ is determined (Step 2) :

$$\mathbb{I}_{var,i} = \mathbb{I}_{var,i} \cup \{t_{var,i+1}\} \quad \text{if } t_{var,i+1} - \max_{t \in \mathbb{I}_{var,i}}(t) \leq b_{intra} \quad (3)$$

3. Any intervals that are too short are integrated into adjacent intervals in the inter-interval regrouping step (step 3) :

$$\mathbb{I}_{var,i+1} = \mathbb{I}_{var,i} \cup \mathbb{I}_{var,i+1} \text{ or } \mathbb{I}_{var,i-1} = \mathbb{I}_{var,i} \cup \mathbb{I}_{var,i-1} \quad \text{if } \max_{t \in \mathbb{I}_{var,i}}(t) - \min_{t \in \mathbb{I}_{var,i}}(t) \leq b_{inter} \quad (4)$$

In the case of adjacent intervals being of different classes, the inter-interval regrouping proceeds depending on its class: if the given interval is of the maximal class, it will be concatenated to the nearest neighbouring inferior class, otherwise it will be added automatically to the nearest superior class interval. These conditions are valid because, from the perspective of the utility operator, it is more convenient to choose the less favourable case in order to limit risks. However, in the first case where up-classing is impossible, the marginality or short duration of fluctuations are assumed to dominate their intensity and the interval is downgraded.

2.2. Optimisation of spatial compensation of solar radiation variations

The phenomenon of spatial compensation of solar radiation variations represents an original alternative to smoothing photovoltaic generation without the need for additional technologies. To this end, optimization of the phenomenon could serve to attenuate variations and provide a relatively stable photovoltaic energy supply over the whole territory.

The optimization problem shall be to find the set of coefficients $(\beta_{S_i})_{i\in[1,N]}$, with $\forall i \in [1,N],\ \beta_{S_i} \geq 0$ and $\sum_{i=1}^{N} \beta_{S_i} = 1$ that minimizes $P_{t,G_{tot}}(C_M)$ the relative cumulated duration of most important variations C_M in the weight sum of global irradiance G_{tot} over all the N sites :

$$G_{tot}(t) = \sum_{i=1}^{N} \beta_{S_i}.G_{S_i}(t) \tag{5}$$

.

So, objective function $F\left((\beta_{S_i})_{i\in[1,N]}\right)$ is :

$$F\left((\beta_{S_i})_{i\in[1,N]}\right) = \min\left(P_{t,G_{tot}}(C_M)\right) \tag{6}$$

The coefficients corresponding to the minimum of the cost function indicate the optimal deployment of photovoltaic capacity at the sites included in the study for a minimum of C_j variations and hence the smoothest possible generation curve.

In order to determine the optimal set of coefficients β_{S_i} an efficient optimisation tool is needed to limit the number of necessary calculations. Ultimately, all combinations $(\beta_{S_i})_{i\in[1,N]}$ should be tested to find the optimal set: for a coefficient precision of 1×10^{-1}, this would entail 9^N tests. Rather than pursing this tedious approach, a genetic algorithm (GA) [36, 37] was employed to accelerate the search.

3. Case study

The methodology developped in section 2 is applied to Corsica Island as it presents characteristics of an good illustrative case study. Indeed, the island can be considered as a non-interconnected zone, since the importation of electricity from the continental grid represents only a fifth of the total grid capacity. As a consequence, the regulatory limit (35 %) of renewable integration in Corsica was reached in 2012 when all existing PV plants were connected to the local grid [38]. The objective of the present work is to highlight and optimize the territorial compensation of solar resource variation as an effective strategy in order

to exceed the regulatory integration limit for intermittent renewables without impacting on the grid. To this end, the spatial and temporal behaviour of solar radiation in Corsica was analysed, using ground-based measurements at a small number of weather stations.

3.1. Geography of the studied territory

Corsica is a Mediterranean island lying in the golf of Genova. From north to south the landmass spans 183 km, from latitude N 41°20′2″ to N 43°1′31″. The island is 83.5 km wide from east to west, covering longitudes E 8°32′30″ to E 9°33′38″. With a surface area of 8722 km^2, Corsica is the fourth largest island in the Mediterranean after Sardinia, Sicily and Cyprus. The island is classed as a "mountain in the sea", with relief above 600 m accounting for 39 % of its surface and an average elevation above sea level of 568 m. Some 120 peaks exceed 2000 m altitude (Rome and Giorgetti, 2007). The coastal regions enjoy a Mediterranean climate characterized by warm, dry summers and mild, humid winters, which translates into a higher solar resource potential than most of metropolitan France. In contrast, in the mountains the climate is strongly affected by the altitude. At the highest altitudes Corsica exhibits an alpine climate. Inland, summers are hot and sunny, but in winter conditions are more unstable with a high degree of precipitation (about 700 mm yr^{-1}). The geographical distribution of the solar potential across the island is therefore particularly heterogeneous and microclimates are present in the region, correlated with elevation as illustrated by the map of daily average radiation in 2005 obtained with processed Meteosat8 satellite images [39].

The geographical dispersion of the studied sites is essential, in order to ensure a representative and coherent dataset for solar radiation across the territory. The positions of the weather stations were therefore carefully chosen taking into account the microclimate zones on the island. The north-eastern and south-western parts of the island do not experience variations in solar radiation at the same time. A line of separation exists, running north-west to south-east due to the orientation of the mountain range in the centre of the island. Coastal areas

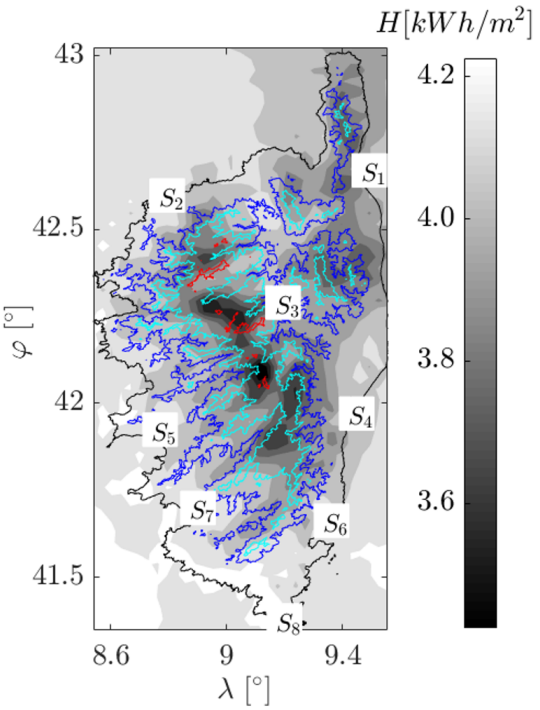

Figure 3: Geographic localisation of measurement stations S_i, micro-climates and elevation contours in Corsica. The greyscale indicates daily irradiation intensity in 2005 over the island. Cyan, blue and red contours highlight the elevation levels at 530 m, 1060 m and 2120 m respectively.

of the north-east and south-west, which represent equivalent microclimates, do not however experience the same weather. It is therefore convenient to install weather stations in both areas. The measurement sites were thus deployed at EDF net interconnection sites, taking into account the above mentioned constraints (Fig. 3), with altitude and geographical coordinates detailed in table 1.

3.2. Dataset

3.2.1. Instrumentation

The apparatus used, SP Lite 2 Kipp & Zonen pyranometers, are equipped with a silicon photodiode of sensitivity 60 to 100 $\mu V\,W^{-1}\,m^{-2}$. Their rapid

Table 1: Geographical coordinates of measures sites

Code	Site	Latitude (φ)	Longitude (λ)	Altitude	N^{er} days
S_1	Lucciana	42°39′49″	9°25′28″	60 m	456
S_2	Calvi	42°33′38″	8°44′48″	31 m	416
S_3	Corte	42°18′4″	9°9′57″	381 m	445
S_4	Ghisonaccia	42°3′54″	9°22′14″	65 m	451
S_5	Ajaccio	41°55′49″	8°45′23″	2 m	355
S_6	Sainte Lucie	41°41′59″	9°20′12″	66 m	405
S_7	Propriano	41°39′43″	8°55′2″	17 m	407
S_8	Bonifacio	41°22′17″	9°12′10″	46 m	450

response time to 95 % signal strength within 1 s allowed for the second-wise measurements undertaken in the current study. This time step was chosen in order to allow a thorough study of short term variations in solar radiation.

3.2.2. Measurement period

The data span a period of 18 months, starting the 24th May 2010 for the stations at Corte and Ajaccio, and a few days later for the other installations. Data acquisition was stopped on the 2nd October 2011. Over the period, occasional service interruptions lasting from a few hours to a few days were experienced. Consequently,

- Some days contain several data gaps, rendering them unusable for the analysis. Those days with more than 10 % missing or unusable data were eliminated from the analysis
- The number and distribution of useable days of data in the dataset vary between sites (Table 1)

Applying the requirement that data from all stations were available (necessary for a comparative analysis), a subset of 152 days was kept for the present analysis. This constraint plus the heterogeneous distribution of the useable dates across the seasons represent serious limiting factors for this type of study. Indeed, the present dataset comprised 62 days in winter, 63 in spring, 21 in summer and only 6 days in autumn. The set of overlapping dates therefore con-

tains a seasonal imbalance, which introduces a statistical bias when comparing sites.

Around the hours of sunrise and sunset the effect of nearby obstructions and airmass result in low radiation intensities. Moreover, these phenomena are deterministic whereas the study is focused on stochastic variation due to cloudy cover. It was therefore necessary to define a so-called energy interval, representing 80 % of the solar energy of the day (at clear sky condition), symmetrical about solar noon and excluding the start and end of each day [40].

3.2.3. Parametrisation of the classification method

The development of the classification method as well as the definition of intervals of variability and of regimes of solar radiation require the determination of four parameters:

1. A variability threshold b_{var} beyond which the conditions are considered fluctuant
2. The values of the variation scales δt used to discriminate the different regimes of solar radiation
3. The thresholds of intra- and inter-intervals regrouping, designated respectively b_{intra} and b_{inter}, which set the limits of the different intervals.

The variability threshold was defined by the french grid operator in Corsica, EDF, which judges a variation to be important when it exceeds 10 % of the radiation received during 5 minutes. It was therefore decided to generalize this 10 % threshold for all of the variability scales to be considered.

The scales of variability δt serve to discriminate variations with different features. It suffices to adopt variation scales that are separated by orders of magnitude in order to discriminate different variation dynamics. Those of order a few seconds may be used to identify deep and narrow variations whereas those of a few minutes, as well as intense variations, recover slow and shallower variations.

Consider $N_{t_{var}}$ the number of instants t_{var} identified, for a given variability scale δt, by the first step of the classification procedure (Fig. 2). Let's define

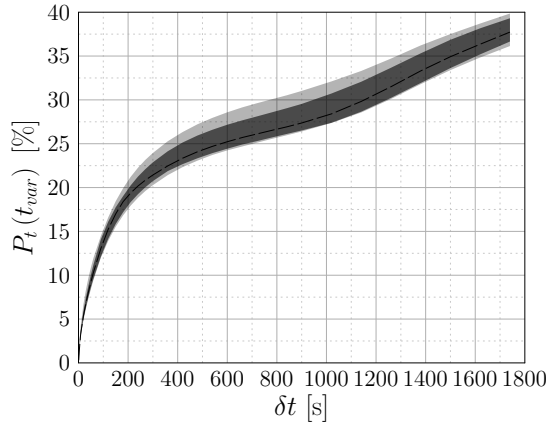

Figure 4: Statistics of $P_t\,(t_{var})$ as a function of the scale of variability δt for the 8 sites on all the study period. The light grey area despicts the range between the 10^{th} and the 90^{th} percentiles, dark grey despicts range between the 25^{th} and the 75^{th} percentiles and dashed line is the median

$P_t\,(t_{var}) = N_{t_{var}}/N_{t_{tot}} * 100$ the ratio of number of variable instants to the total sample of the measurement period $N_{t_{tot}}$. $P_t\,(t_{var})$ can be seen as the cumulative time variable on the whole sample.

On figure 4, we can observe that the ranges between 25^{th} and the 75^{th} of $P_t\,(t_{var})$ and its derivative drawn a thick envelope curves. It shows that whatever the site, $P_t\,(t_{var})$ has the same shape: $P_t\,(t_{var})$ increases with the scale of variations δt considered. More precisely, $P_t\,(t_{var})$ rises rapidly up until an inflexion of the envelop, for $\delta t = 300\,\text{s}$. Very fewer variable instants are found for $\delta t = 1\,\text{s}$ than for $\delta t = 300\,\text{s}$. These points reflect different types of variations to those observed for $\delta t = 300\,\text{s}$: large variation scales can be used to identify slow variations in addition to deep and fast found with small scales. Then, we can see $P_t\,(t_{var})$ increases slowly for $\delta t \geq 300\,\text{s}$ and $\delta t \leq 1200\,\text{s}$: nearly the same instants are considered variable when δt is set in this intervale of values. Finaly, more variations identified at $\delta t > 1200\,\text{s}$. These additionalvariations are not directly associated to meteorological instabilities, but rather may arise from the variation in solar radiation under clear sky conditions.

From this analysis of figure 4, it appears appropriate to undertake an analysis considering two variation scales, $\delta t_1 = 1\,\mathrm{s}$ and $\delta t_2 = 300\,\mathrm{s}$, used to define three classes:

- Class 0 (C_0): stable conditions, with no visible variations for $\delta t = 1\,\mathrm{s}$ or $\delta t = 300\,\mathrm{s}$;
- Class 1 (C_1): slow and shallow variations perceptible only for $\delta t = 300\,\mathrm{s}$;
- Class 2 (C_2): narrow and deep variations present for both scales, $\delta t = 1\,\mathrm{s}$ and $\delta t = 300\,\mathrm{s}$.

The roles of b_{intra} and b_{inter} are equivalent: b_{intra} can be interpreted as a maximal time interval between two variations, and therefore the minimum size of stable intervals; whereas the b_{inter} designates the minimum size of variable intervals. These thresholds therefore represent the minimal sizes of intervals, stable or otherwise, and hence it is appropriate to consider identical values for the two parameters.

Figure 5 presents intervals delimited for different regrouping thresholds, which are observed to as significant an impact on the data as the configurations, when the thresholds are varied from $b_{intra} = b_{inter} = 1\,\mathrm{s}$ to $b_{intra} = b_{inter} = 300\,\mathrm{s}$, $b_{intra} = b_{inter} = 900\,\mathrm{s}$ and finally to $b_{intra} = b_{inter} = 1800\,\mathrm{s}$.

As was previously expected, without regrouping ($b_{intra} = b_{inter} = 1\,\mathrm{s}$) a large number of small discontinuous intervals are observed (Fig.5(a)). The application of these thresholds serves to eliminate marginal variations. Thus, all unstable points classified as C_1 observed between 10:28 and 10:33 (Fig.5(a)) change to C_0 when regrouping is applied (Fig.5(b), 5(c) et 5(d)). The intervals generated by the instabilities during these times do not exceed the threshold Sinter, and are therefore declassified.

These thresholds are responsible for a considerable restructuring of the variation intervals. Therefore,

- Data belonging to C_2 between 1:40 pm and 2:00 pm before regrouping are too spaced out to be regrouped into an interval when $b_{intra} = b_{inter} =$

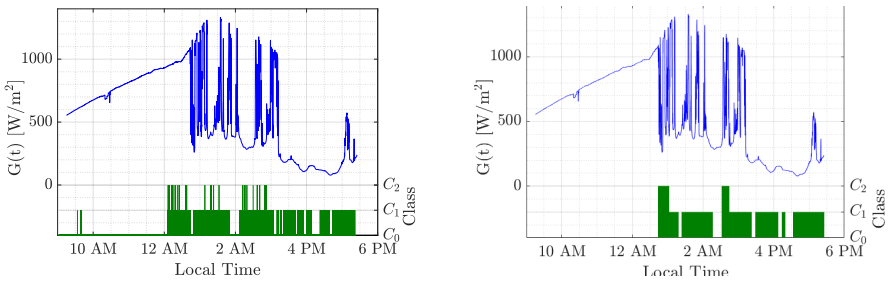

(a) $S_{intra} = S_{inter} = 1\,\text{s}$

(b) $S_{intra} = S_{inter} = 300\,\text{s}$

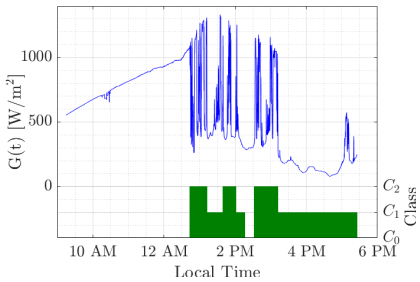

(c) $S_{intra} = S_{inter} = 900\,\text{s}$

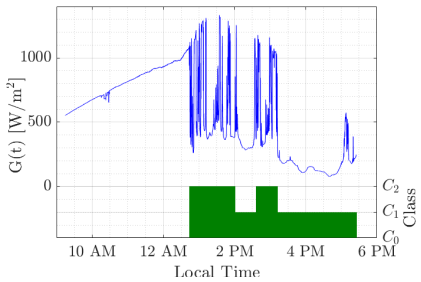

(d) $S_{intra} = S_{inter} = 1200\,\text{s}$

Figure 5: Intervals revealed for a variability threshold of 10 %, $dt_1 = 1\,\text{s}$ and $dt_2 = 300\,\text{s}$ and different values of intra and inter – interval grouping thresholds

300 s, and are thus declassified (Fig.5(b)). In contrast, the same points are regrouped into an interval of class C_2 for $b_{intra} = b_{inter} = 900\,\text{s}$ (Fig.5(c)). Finally, they integrate class C_2 interval between 12:25 pm and 1:12 pm when $b_{intra} = b_{inter} = 900\,\text{s}$ (Fig.5(d)).

- Points classed as C_2 for the range 2:36 pm to 2:43 pm are retained in this class when $b_{intra} = b_{inter} = 300\,\text{s}$, because the subsequent points are two spread out to be included. These points are retained within this interval when the thresholds are raised to $b_{intra} = b_{inter} = 900\,\text{s}$ and $b_{intra} = b_{inter} = 1800\,\text{s}$.

We can observe a total of 14 intervals were identified for $b_{intra} = b_{inter} = 300\,\text{s}$ (Fig. 5(b)), of which 6 persist less than 15 minutes. For $b_{intra} = b_{inter} = 900\,\text{s}$ (Fig. 5(c)), 8 intervals are recovered, whereas 5 are found for regrouping

thresholds of 1800 s (Fig. 5(d)). It should be noted that a period in which N intervals are identified for $b_{intra} = b_{inter} = 300\,\mathrm{s}$, including M intervals of durations shorter than 900 s, will not be split into $N - M$ intervals when considering $b_{intra} = b_{inter} = 900\,\mathrm{s}$.

Overall, the smaller the thresholds, the larger the degree of segmentation of days and the smaller the intervals hat will be obtained (Fig. 4). With this in mind, and in the absence of any objective criterion for the determination of these thresholds, they should rather be set be according to the specific application under study, the subsequent analysis, and the desired temporal resolution needed for that application.

4. Results and discussion

4.1. Characterisation of fluctuations observed at each site

The method introduced in section 2 was implemented to characterise the fluctuations observed at the 8 sites, considering a variability threshold of b_{var} = 10 %, and two scales of variations $\delta t_1 = 1\,\mathrm{s}$ and $\delta t_2 = 300\,\mathrm{s}$ to allow the evaluation of the three classes defined above. The thresholds intra- and inter-regrouping were set to $b_{intra} = b_{inter} = 900\,\mathrm{s}$, affording a good compromise between temporal resolution for intervals and the number of intervals to be defined. This comparative assessment was undertaken using the 152 days of overlapping data.

The results of this comparative analysis of intervals are shown in figure 6, where each class C_j is presented with its associated weight in terms of

1. relative cumulated durations $P_t\,(C_j)$ of intervals, obtained by evaluating the number of measurements associated to each class relative to the sample size.
2. relative number of intervals $P_N\,(C_j)$, obtained by counting the amount of interval of each class normalized by the total amount of intervals.

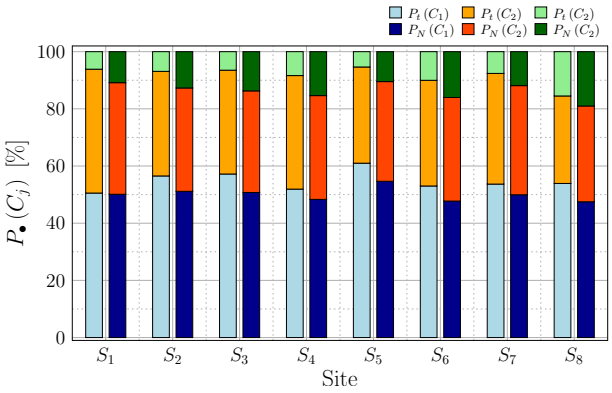

Figure 6: Histograms of relative numbers of intervals $P_N\,(C_j)$ and relative cumulated durations $P_t\,(C_j)$ of variation class C_j for the studied sites S_i

The fluctuations of all stations exhibit $P_t\,(C_0) > P_N\,(C_0)$, and with the exception of Ajaccio (S_5) and Bonifacio (S_8), $P_t\,(C_1) > P_N\,(C_1)$. These observations show that the intervals of classes C_0 and C_1 tend to be relatively long. For example, 50 % of the intervals of class C_0 at Propriano (S_7) represent some 53.7 % of the measurement time; similarly, 36.3 % of the intervals classed C_1 at Ghisonaccia (S_4) occupy 39.7 % of the time. In contrast, $P_t\,(C_2) < P_N\,(C_2)$ indicates that the intervals of class C_2 tend to be of short duration. One observes that at the Lucciana site (S_1) for example, 10.9 % of the intervals represent 6.13 % of the measurement time.

Ajaccio (S_5) appears to be meteorologically the most stable of the 8 sites, with the most intervals of class C_0 and the fewest of class C_2 which is confirmed in terms of the cumulated time: variations of class C_0 represent 61 % of the period whereas class C_2 covers only 5.36 % (Fig.6). At the other extreme, Bonifacio (S_8) experiences the least stable conditions with a larger frequency of C_2 variations, representing 19 % of intervals and 15.5 % of cumulated time.

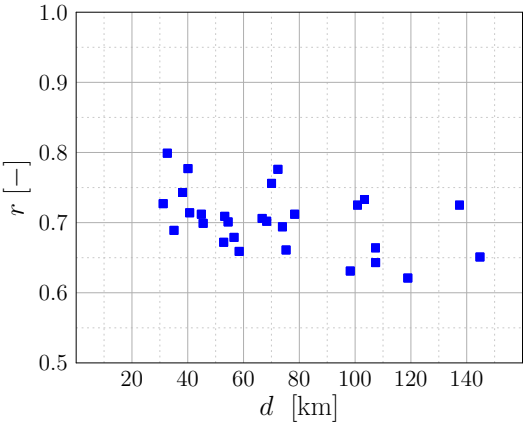

Figure 7: Variagramm of the irradiance data per paire of sites: standard variations between irradiances measured over paire of sites as a function of distances

4.2. Characterising the spatial compensation of the solar resource in Corsica

4.2.1. Evidence for the phenomenon

The subset of data corresponding to daylight hours was retained for the comparative analysis. Pair-wise linear correlation coefficients were evaluated for the 152 days of overlapping data for each weather stations and the seven other sites. As can be seen in figure 7, the correlation factor between sites was found to not exceed 0.8 for the available data, indicating that the sites are not strongly correlated. The data exhibit phase differences between the variations observed from one site to the next, which therefore may be exploited to smooth the effects of intermittence and hence take advantage of the spatial compensations of the solar resource.

With the aid of the present data analysis, it has been possible to draw certain observations of the spatial compensation of the solar resource that are nevertheless indicative of the presence of the phenomenon for Corsica.

- Distinct variations in meteorological conditions recorded as a function of geographical position;
- correlation coefficients not exceeding 0.8 between sites (Fig.7), arising from

phase shifts in cloud phenomena;

- Different fluctuations observed by the classification method, indicating different climate and weather from one site to another.

Also, we can observe that the degree of fluctuation observed for individual sites (Fig. 8(a), 8(b), 8(c), 8(d), 8(e), 8(f), 8(g), 8(h)) is attenuated when the solar radiation is integrated over all sites (Fig. 8(i)). For instance, some sites exhibit significant variations in solar radiation during the afternoon: such variations of class C_2 were observed in Lucciana (S_1), Calvi (S_2) and Bonifacio (S_8). These variations are attenuated when considering the average, and none of them are of class C_1. These observation are consistent with earlier evidence.

The distribution of solar radiation over the island is therefore favourable to concept of territorial smoothing of the solar resource, although it remains necessary to develop a more general proof for all days and also a method to quantify the level of compensation achieved. Conventional statistical methods such as histograms of variations are inadequate for the current study. Indeed, we have not found any suitable data representation tool to visualise and quantify the variations. The use of variation classes could serve to prove the existence of the phenomenon, by presenting the class distribution for individual sites and the cumulated signal.

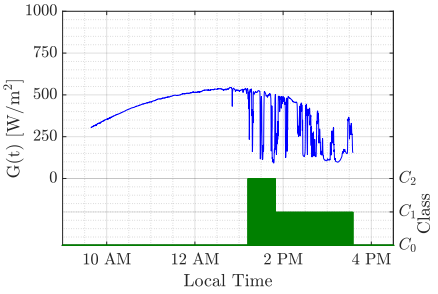

(a) S_1: Lucciana

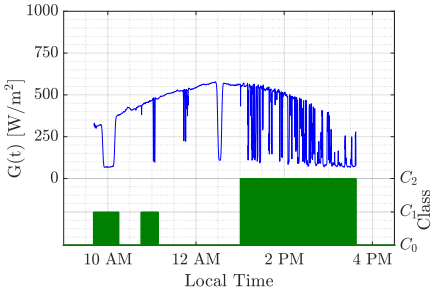

(b) S_2 : Calvi

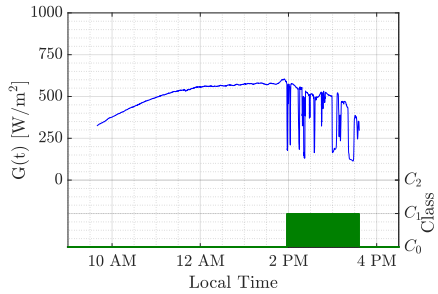

(c) S_3 : Corte

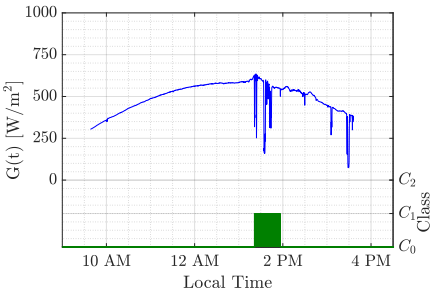

(d) S_4 : Ghisonaccia

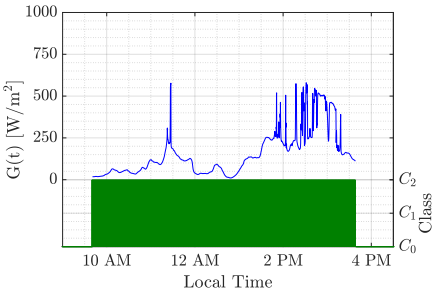

(e) S_5 : Ajaccio

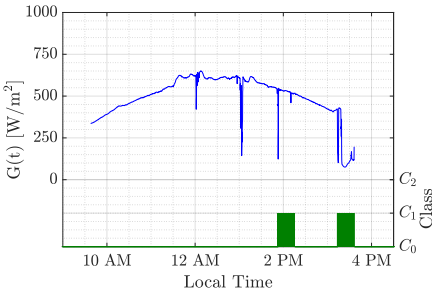

(f) S_6 :Sainte Lucie

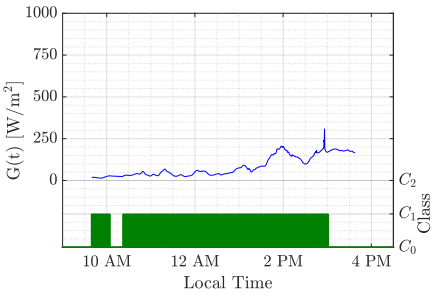

(g) S_7 Propriano

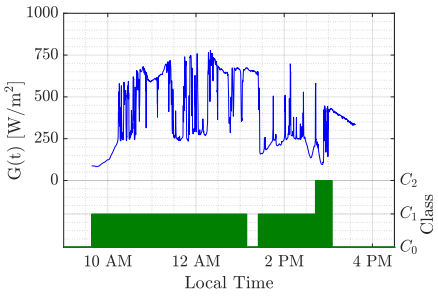

(h) S_8 Bonifacio

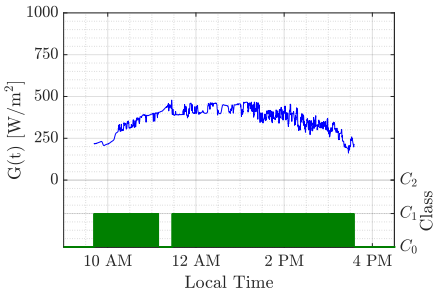

(i) Average

Figure 8: Irradiances and variations classes ($b_{var} = 10$ %, $\delta t_1 = 1$ s, $\delta t_2 = 300$ s, and $b_{intra} = b_{inter} = 900$ s) over the sites and average, on 13$^{\text{th}}$ February 2011

4.2.2. Quantification of spatial compensation

In the present work, the durations of intervals associated to the various classes has been used to characterize the phenomenon of territorial smoothing, by classifying the solar radiation at each site and then studying the cumulated duration of each class. The integrated radiation over all sites can be analysed following the same procedure. This method was applied to the 152 days of overlapping data for the 8 sites, using the same parameters as the analysis of individual sites: $b_{var} = 10$ %, $\delta t_1 = 1$ s, $\delta t_2 = 300$ s, and $b_{intra} = b_{inter} = 900$ s, and hence the same three class descriptions. Recall that, for all sites, the class C_0 variations are the most frequent, representing some 50 – 60 % of the study period, whereas class C_1 variations account for 30 – 40 %. Class C_2 variations are the least common, covering only 5 – 15 % of the measurement time (Fig.

6). When the data are cumulated over all sites, class C1 variations increase at the expense of the other classes (Fig. 9).

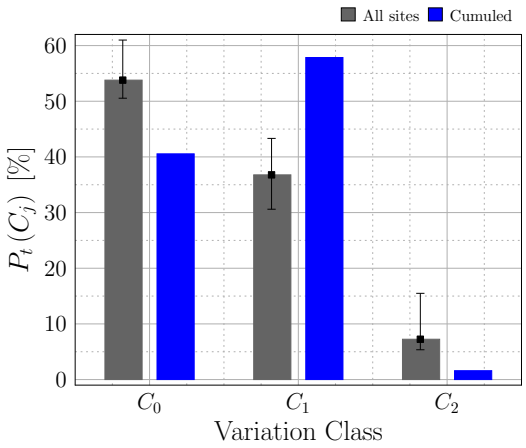

Figure 9: Relative cumulated durations of intervals $P_t(C_j)$ of each class C_j considering the individual sites in gray histograms (the errorbar depicts the minimal and maximal values all sites considered) and the accumulation of the global radiation over all the sites, illustrating territorial compensation in blue histograms

This result shows firstly that C_2 variations are smoothed and become less frequent when radiation is integrated over several sites : only 1.7 % of the cumulated dataset is associated to class C_2 compared to 5.36 % for the most favourable site. Else, an increase of cumulated duration of C_1 intervals is observed, whereas C_0 intervals duration decreases slighly. This undesired growth of $C1$ interval cumumated time can be explained by considering that C_2 variations may be smoothed through the summation of either C_2 variations that are out of phase, or C_0 variations that attenuate the relative fluctuations. For the latter case, C_0 variation are transformed to C_1. Despite this, the overall effect is to smooth the radiation trend.

4.2.3. Optimisation results

A simple GA was implemented to determine the coefficients $(\beta_{S_i})_{i\in[1,8]}$ for a range of tests, which converged after 70 to 75 generations of 20 individuals. The obtained coefficients are summarized in table 2. They are the result of 8

applications of the GA on the scale of the study, the calculations being reiterated in order to test the sensitivity of the coefficients and thus exclude the hypothesis of a given solution corresponding to a local minimum.

Table 2: β_i coefficients for each site S_i, with their uncertainties obtained with GA optimization ran 8 times

Code	Sites	β_{S_i} [%]
S_1	Lucciana	26.04 ± 1.80 %
S_2	Calvi	11.71 ± 0.65 %
S_3	Corte	16.20 ± 2.47 %
S_4	Ghisonaccia	8.40 ± 0.73 %
S_5	Ajaccio	16.51 ± 2.01 %
S_6	Sainte Lucie	5.29 ± 0.33 %
S_7	Propriano	12.55 ± 0.57 %
S_8	Bonifacio	2.81 ± 0.47 %

Operationnally, the β_i coefficients can be translated as rates of the total PV capacity installed on the territory to be implemented at around each site. Thus, a map of the optimal dispersion of PV installations is shown in figure 10.

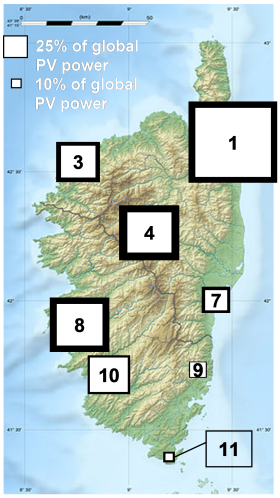

Figure 10: Territorial redistribution of solar electricity generation for an optimal compensation of variations. The sizes of the squares denote the optmial rate of PV global capacity on the site zone and the thickness of the edges represent the uncertainties of the optimization

Those sites with the least C_2 variations are found to carry the greatest

weight: the Lucciana and Ajaccio sites, with C_2 variations covering 6.13 % and 5.29 % of time respectively, have weights of 26.04 ± 1.80 % and 16.51 ± 2.01 %. Reciprocally the most unstable site, Bonifacio, was designated the smallest coefficient of 2.81 ± 0.47%. The optimization process had two positive outcomes (Fig. 11):

- The near total suppression of C_2 variations, which after optimisation account for only 0.13% of the measurement period of 6600 s;
- A reduction in the growth in frequency of C_1 variations. The occurrence of this class of variation was limited to a level comparable to the site with the highest frequency of C_1 variations.

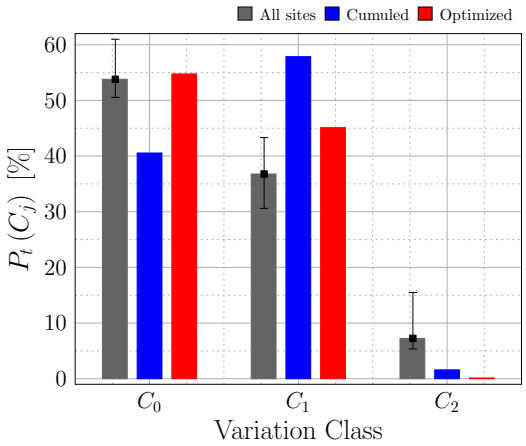

Figure 11: Relative cumulated durations of intervals $P_t\,(C_j)$ of each class C_j considering the individual sites in gray histograms (the errorbar depicts the minimal and maximal values all sites considered) ; the accumulation of the global radiation over all the sites, illustrating territorial compensation in blue histograms and the compensations phenomenon optimization in red histograms

The ratios of points considered unstable relative to the number of data, for the sample of 152 days, are for any interval in the range $dt \in [1; 1800]$ less for the spatially compensated combinations than for the individual sites (Fig.12(a)).

The optimization improves on the simple sum of irradiances by reducing

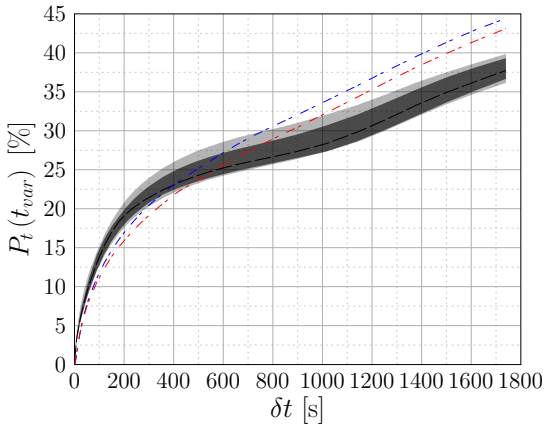

(a) $1 \leq dt \leq 1800\,\mathrm{s}$

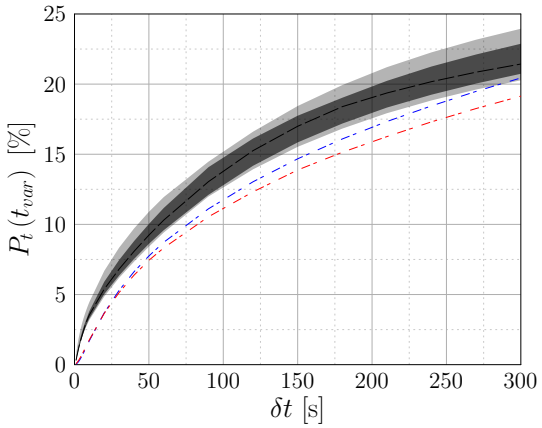

(b) $1 \leq dt \leq 60\,\mathrm{s}$

Figure 12: Proportion of unstable periods to the total data sample for the 8 sites; for the territorial variation compensations (blue) and the optimized case (red)

the number of strong variations for scales from 1 to 20 s. Smaller variations, for scales greater than 20 s, are less impacted by the optimization search (Fig.12(b)). This is explained by the fact that the optimization processes is focused more towards the larger variations because the criterion to minimize is the number of variations observable at 1 s. In general, the smoothing afforded for this type of variation can only be partial, hence strong variations are downgraded to moderate ones, which are observable for larger scales and thus the ratio for these scales increases.

5. Conclusion

We have presented in this paper a new typological classification method for solar radiation, in which the principle innovation resides in the decomposition of days into intervals of different classes according the regime of solar radiation and its variability.

This classification method has been applied to the meteorological characterization of sites across the territory of Corsica, and in order to demonstrate the phenomenon of spatial compensation through an understanding of variations: the collection of events for which the variations were sufficiently important to be classified "strong variations" is limited when radiation is integrated across several sites. Therefore, the observable fluctuations at the scale of 1 s, classed C_2, represent between 5.5 and 15.5 % of the measured time for individual sites whereas they represent 1.7 % for the cumulated intensity.

A genetic algorithm was subsequently implemented in order to optimise the compensation afforded by spatially distributed radiation, and was found able to practically eliminate intervals of strong variation. Variations of class C_2 represented only 0.13 % after optimization.

However, even once optimised, the compensation is not complete for the set of sites under consideration, and some variations were found to persist. Therefore in the case of a high degree of penetration of intermittent renewable energy resources in Corsica, the utility operator will always need to manage the

variations and thus overcome the intermittence of energy generation in order to ensure the stability of the grid supply and guaranty the electricity service.

References

[1] P. Haurant, P. Oberti, M. Muselli, Multicriteria selection aiding related to photovoltaic plants on farming fields on Corsica island: A real case study using the ELECTRE outranking framework, Energy Policy 39 (2) (2011) 676–688. doi:10.1016/j.enpol.2010.10.040.
URL http://linkinghub.elsevier.com/retrieve/pii/S0301421510007913

[2] P. Oberti, M. Muselli, P. Haurant, Photovoltaic Plants Selection on an Insular Grid Using Multicriteria Outranking Tools: Application in Corsica Island (France), in: F. Cavallaro (Ed.), Assessment and Simulation Tools for Sustainable Energy Systems, Vol. 129, Springer London, London, 2013, pp. 27–54.

[3] A. Woyte, V. V. Thong, R. Belmans, J. Nijs, Voltage fluctuations on distribution level introduced by photovoltaic systems, IEEE Transactions on Energy Conversion 21 (1) (2006) 202–209. doi:10.1109/TEC.2005.845454.

[4] P. Denholm, R. M. Margolis, Evaluating the limits of solar photovoltaics (PV) in traditional electric power systems, Energy Policy 35 (5) (2007) 2852 – 2861. doi:https://doi.org/10.1016/j.enpol.2006.10.014.
URL http://www.sciencedirect.com/science/article/pii/S0301421506003740

[5] J. Paatero, P. Lund, Effects of large-scale photovoltaic power integration on electricity distribution networks, Renewable Energy 32 (2) (2007) 216–234. doi:10.1016/j.renene.2006.01.005.
URL https://linkinghub.elsevier.com/retrieve/pii/S0960148106000425

[6] M. Eltawil, Z. Zhao, Grid-connected photovoltaic power systems: Technical and potential problems—A review, Renewable and Sustainable Energy Reviews 14 (1) (2010) 112–129. doi:10.1016/j.rser.2009.07.015.

URL https://linkinghub.elsevier.com/retrieve/pii/S1364032109001749

[7] J.O, Décret n° 2015-1697 du 18 décembre 2015 relatif à la programmation pluriannuelle de l'énergie de Corse (Dec. 2015).

[8] J.O, Décret n° 2017-530 du 12 avril 2017 relatif à la programmation pluriannuelle de l'énergie de la réunion (Apr. 2017).

[9] R. Perez, M. David, T. E. Hoff, M. Jamaly, S. Kivalov, J. Kleissl, P. Lauret, M. Perez, Spatial and temporal variability of solar energy, Foundations and Trends® in Renewable Energy 1 (1) (2016) 1–44. doi:10.1561/2700000006.
URL http://dx.doi.org/10.1561/2700000006

[10] H. Gallegos, R. Lopardo, Spatial variability of the global solar radiation obtained by the solarimetric network in the Argentine Pampa Humeda, Solar Energy 40 (5) (1988) 397–404. doi:10.1016/0038-092X(88)90094-1.
URL https://linkinghub.elsevier.com/retrieve/pii/0038092X88900941

[11] C. Gueymard, S. Wilcox, Assessment of spatial and temporal variability in the US solar resource from radiometric measurements and predictions from models using ground-based or satellite data, Solar Energy 85 (5) (2011) 1068–1084. doi:10.1016/j.solener.2011.02.030.
URL http://linkinghub.elsevier.com/retrieve/pii/S0038092X11000855

[12] M. David, F. Andriamasomanana, O. Liandrat, Spatial and Temporal Variability of PV Output in an Insular Grid: Case of Reunion Island, Energy Procedia 57 (2014) 1275–1282. doi:10.1016/j.egypro.2014.10.117.
URL http://linkinghub.elsevier.com/retrieve/pii/S1876610214014842

[13] C. Glasbey, R. Graham, A. Hunter, Spatio-temporal variability of solar energy across a region : statistical modelling approach, Solar Energy 70 (4) (2001) 373–381.

[14] R. Perez, S. Kivalov, T. Hoff, Spatial & Temporal Characteristics of Solar Radiation Variability, in: Proceedings of the ISES Solar World Congress 2011, International Solar Energy Society, Kassel, Germany, 2011, pp. 1–11. doi:10.18086/swc.2011.24.23.
URL http://proceedings.ises.org/citation?doi=swc.2011.24.23

[15] J. Badosa, M. Haeffelin, H. Chepfer, Scales of spatial and temporal variation of solar irradiance on Reunion tropical island, Solar Energy 88 (2013) 42–56. doi:10.1016/j.solener.2012.11.007.
URL https://linkinghub.elsevier.com/retrieve/pii/S0038092X12003982

[16] T. E. Hoff, R. Perez, Quantifying PV power Output Variability, Solar Energy 84 (10) (2010) 1782–1793. doi:10.1016/j.solener.2010.07.003.
URL https://linkinghub.elsevier.com/retrieve/pii/S0038092X10002380

[17] M. Lave, J. Kleissl, Solar variability of four sites across the state of Colorado, Renewable Energy 35 (12) (2010) 2867–2873. doi:10.1016/j.renene.2010.05.013.
URL https://linkinghub.elsevier.com/retrieve/pii/S0960148110002314

[18] K. Otani, J. Minowa, K. Kurokawa, Study on areal solar irradiance for analyzing areally-totalized PV systems, Solar Energy Materials and Solar Cells 47 (1) (1997) 281 – 288. doi:https://doi.org/10.1016/S0927-0248(97)00050-0.
URL http://www.sciencedirect.com/science/article/pii/S0927024897000500

[19] J. Marcos, L. Marroyo, E. Lorenzo, D. Alvira, E. Izco, Power output fluctuations in large scale pv plants: One year observations with one second resolution and a derived analytic model, Progress in Photovoltaics: Research and Applications 19 (2) (2011) 218–227. doi:10.1002/pip.1016.
URL http://doi.wiley.com/10.1002/pip.1016

[20] B. Urquhart, M. Sengupta, J. Keller, Optimizing Geographic Allotment of Photovoltaic Capacity in a Distributed Generation Setting, in: 27th European Photovoltaic Solar Energy Conference and Exhibition, Frankfurt, Germany, 2012.

[21] W. T. Jewell, T. D. Unruh, Limits on cloud-induced fluctuation in photovoltaic generation, IEEE Transactions on Energy Conversion 5 (1) (1990) 8–14. doi:10.1109/60.50805.

[22] R. Collins, K. Crowther, Systems-based modeling of generation variability under alternate geographic configurations of photovoltaic (PV) installations in Virginia, Energy Policy 39 (10) (2011) 6262–6270. doi:10.1016/j.enpol.2011.07.025.
URL https://linkinghub.elsevier.com/retrieve/pii/S0301421511005490

[23] J. Marcos, I. de la Parra, M. García, L. Marroyo, Simulating the variability of dispersed large PV plants: Simulating the variability of dispersed large PV plants, Progress in Photovoltaics: Research and Applications 24 (5) (2016) 680–691. doi:10.1002/pip.2719.
URL http://doi.wiley.com/10.1002/pip.2719

[24] C. Rigollier, M. Lefèvre, L. Wald, The method Heliosat-2 for deriving shortwave solar radiation from satellite images, Solar Energy 77 (2) (2004) 159–169. doi:10.1016/j.solener.2004.04.017.
URL http://www.sciencedirect.com/science/article/B6V50-4CMHKPM-1/2/9eee0d4079bad5382ff4287b96487a2a

[25] A. Mefti, A. Adane, M. Bouroubi, Satellite approach based on cloud cover classification: Estimation of hourly global solar radiation from meteosat images, Energy Conversion and Management 49 (4) (2008) 652–659. doi:10.1016/j.enconman.2007.07.041.
URL http://www.sciencedirect.com/science/article/B6V2P-4PMYX8X-3/2/e19170e0fc0ff16cdbaff933e20d500a

[26] G. Notton, C. Cristofari, M. Muselli, P. Poggi, Calculation on an hourly basis of solar diffuse irradiations from global data for horizontal surfaces in Ajaccio, Energy Conversion and Management 45 (18-19) (2004) 2849–2866. doi:10.1016/j.enconman.2004.01.003.
URL http://www.sciencedirect.com/science/article/B6V2P-4BVRNP6-1/2/e92520f0e770a9b1d8713881b48ce66e

[27] A. de Miguel, J. Bilbao, R. Aguiar, H. Kambezidis, E. Negro, Diffuse solar irradiation model evaluation in the North Mediterranean Belt area, Solar Energy 70 (2) (2001) 143–153. doi:16/S0038-092X(00)00135-3.
URL http://www.sciencedirect.com/science/article/pii/S0038092X00001353

[28] D. Li, J. Lam, An analysis of climatic parameters and sky condition classification, Building and Environment 36 (4) (2001) 435 – 445. doi:https://doi.org/10.1016/S0360-1323(00)00027-5.
URL http://www.sciencedirect.com/science/article/pii/S0360132300000275

[29] A. Maafi, S. Harrouni, Preliminary results of the fractal classification of daily solar irradiances, Solar Energy 75 (1) (2003) 53 – 61. doi:https://doi.org/10.1016/S0038-092X(03)00192-0.
URL http://www.sciencedirect.com/science/article/pii/S0038092X03001920

[30] S. Harrouni, A. Guessoum, A. Maafi, Classification of daily solar irradiation by fractional analysis of 10-min-means of solar irradiance, The-

oretical and Applied Climatology 80 (1) (2005) 27–36. doi:10.1007/s00704-004-0085-0.
URL https://doi.org/10.1007/s00704-004-0085-0

[31] T. Soubdhan, R. Emilion, R. Calif, Classification of daily solar radiation distributions using a mixture of Dirichlet distributions, Solar Energy 83 (7) (2009) 1056–1063. doi:10.1016/j.solener.2009.01.010.
URL https://linkinghub.elsevier.com/retrieve/pii/S0038092X09000073

[32] A. Woyte, R. Belmans, J. Nijs, Fluctuations in instantaneous clearness index: Analysis and statistics, Solar Energy 81 (2) (2007) 195 – 206. doi:https://doi.org/10.1016/j.solener.2006.03.001.
URL http://www.sciencedirect.com/science/article/pii/S0038092X0600079X

[33] P. Jeanty, M. Delsaut, H. Ralambondrainy, J. Lan-Sun-Luk, M. Dessafy, P. Charton, J. Chabriat, Clustering daily solar radiation from Reunion Island using data analysis methods, in: Renewable Energy and Power Quality Journal, Renewable Energy and Power Quality Journal, Bilbao, Spain, 2013, p. 6.

[34] M. Muselli, P. Poggi, G. Notton, A. Louche, Classification of typical meteorological days from global irradiation records and comparison between two Mediterranean coastal sites in Corsica Island, Energy Conversion 41 (10) (2000) 1043–1063.

[35] P. Haurant, A. Rodler, G.-A. Faggianelli, M. Muselli, P. Poggi, Intermittence forecasting of the solar resource in Corsica, International Solar Energy Society, Daegu, 2015, pp. 1–11. doi:10.18086/swc.2015.07.03.
URL http://proceedings.ises.org/citation?doi=swc.2015.07.03

[36] J. Holland, Adaptation in Natural and Artificial Systems, MIT Press, Cambridge, MA, USA, 1975.

[37] D. Goldberg, Genetic algorithms in search, Optimization, and Machine-Learning (1989).
URL https://ci.nii.ac.jp/naid/10000038763/en/

[38] EDF, Bilan prévisionnel de l'equilibre offre/demande d'électricité corse, Tech. rep., EDF SEI (2011).

[39] P. Haurant, M. Muselli, B. Pillot, P. Oberti, Disaggregation of satellite derived irradiance maps: Evaluation of the process and application to Corsica, Solar Energy 86 (11) (2012) 3168–3182. doi:10.1016/j.solener.2012.08.010.
URL http://www.sciencedirect.com/science/article/pii/S0038092X12003015

[40] P. Haurant, De la sélection multicritère de parcs photovoltaïques à la cartographie et l'étude de l'intermittence de la ressource : modélisations appliquées à l'île de Corse, Ph.D. thesis, Université de Corse Pascal Paoli, Ajaccio (2012).